

Biological activities of 7-dehydrocholesterol-derived oxysterols: implications for Smith-Lemli-Opitz syndrome[§]

Zeljka Korade,^{2,††} Libin Xu,^{2,†} Richard Shelton,^{††} and Ned A. Porter^{1,†}

[†]Department of Chemistry and Vanderbilt Institute of Chemical Biology, ^{††}Department of Psychiatry and Vanderbilt Kennedy Center for Research on Human Development, Vanderbilt University, Nashville, TN 37235

Abstract Smith-Lemli-Opitz syndrome (SLOS) is a metabolic and developmental disorder caused by mutations in the gene encoding the enzyme 7-dehydrocholesterol reductase (Dhcr7). This reductase catalyzes the last step in cholesterol biosynthesis, and levels of 7-dehydrocholesterol (7-DHC), the substrate for this enzyme, are elevated in SLOS patients as a result of this defect. Our group has previously shown that 7-DHC is extremely prone to free radical autoxidation, and we identified about a dozen different oxysterols formed from oxidation of 7-DHC. We report here that 7-DHC-derived oxysterols reduce cell viability in a dose- and time-dependent manner, some of the compounds showing activity at sub-micromolar concentrations. The reduction of cell survival is caused by a combination of reduced proliferation and induced differentiation of the Neuro2a cells. The complex 7-DHC oxysterol mixture added to control Neuro2a cells also triggers the gene expression changes that were previously identified in Dhcr7-deficient Neuro2a cells. Based on the identification of overlapping gene expression changes in Dhcr7-deficient and 7-DHC oxysterol-treated Neuro2a cells, we hypothesize that some of the pathophysiological findings in the mouse SLOS model and SLOS patients might be due to accumulated 7-DHC oxysterols.—Korade, Z., L. Xu, R. Shelton, and N. A. Porter. Biological activities of 7-dehydrocholesterol-derived oxysterols: implications for Smith-Lemli-Opitz syndrome. *J. Lipid Res.* 51: 3259–3269.

Supplementary key words gene expression • free radical oxidation • lipid peroxidation

Lipids, including cholesterol, 7-dehydrocholesterol (7-DHC), and PUFAs, are prone to undergo reactions with molecular oxygen by free radical mechanisms (1–3). This process, known as lipid peroxidation, gives rise to a host of

peroxide products (1–6). Over the past several years, we have determined the rate constants for lipid peroxidation of PUFAs, and, because of their importance in mammalian biology, we recently determined the propagation rate constants for cholesterol and 7-DHC (7). The rate constant for cholesterol, $11 \text{ M}^{-1}\text{s}^{-1}$, falls in line with those determined for other cycloalkenes, with cyclohexene and cyclopentene both having values of about $6 \text{ M}^{-1}\text{s}^{-1}$ (8). On the other hand, the constant determined for autoxidation of 7-DHC, $2,260 \text{ M}^{-1}\text{s}^{-1}$, is surprisingly large, and this rate constant makes 7-DHC the most reactive organic compound that can maintain an oxidative free radical chain reaction (7).

Accumulation of 7-DHC in tissues and fluids is observed in patients with Smith-Lemli-Opitz Syndrome (SLOS) (9–11). SLOS results from mutations in the gene encoding the last enzyme of the cholesterol biosynthesis pathway, 7-DHC reductase (Dhcr7) (12–15). The SLOS mutations lead to inactivation of the Dhcr7 enzyme, resulting in elevated levels of 7-DHC and reduced levels of cholesterol (10, 11, 16). Typical clinical features of SLOS patients include a distinctive facial appearance, cleft palate, and limb anomalies, syndactyly of the second and third toes being the most frequent one observed (17, 18). Nervous system abnormalities include microcephaly, myelin maturation delay, lysencephaly, agenesis/hypoplasia of the corpus callosum, hypoplastic cerebellum, and other central nervous system deficits (17, 18). Clinically, nervous system abnormality manifestations are extremely broad, from minor learning and behavioral problems to mental retardation and autism-like symptoms (19, 20).

It is not clear if these abnormalities arise as a result of cholesterol deficiency, increased levels of 7-DHC, or other

This work was supported by the National Institutes of Health (ES-013125), the National Science Foundation (CHE 0717067), and the Vanderbilt Center for Molecular Toxicology Center (grant NIH P30 ES000267). Its contents are solely the responsibility of the authors and do not necessarily represent the official views of the National Institutes of Health.

Manuscript received 21 June 2010 and in revised form 11 August 2010.

Published, JLR Papers in Press, August 10, 2010

DOI 10.1194/jlr.M009365

Abbreviations: 7-DHC, 7-dehydrocholesterol; Dhcr7, 7-dehydrocholesterol reductase; LXR, liver X receptor; qPCR, quantitative PCR; SLOS, Smith-Lemli-Opitz syndrome; UV, ultraviolet.

²Z. Korade and L. Xu contributed equally to this work.

[†]To whom correspondence should be addressed.

e-mail: n.porter@vanderbilt.edu

[§]The online version of this article (available at <http://www.jlr.org>) contains supplementary data in the form of five figures.

mechanisms. One hypothesis is that 7-DHC and/or its oxidative derivatives, i.e., oxysterols, are biologically active, which may play some role in the pathology of SLOS (19, 21–24). In one recent study, for example, it was reported that high levels of 7-DHC cause exaggerated photosensitivity to ultraviolet (UV) A for SLOS patients (24). Long-wavelength UV irradiation has been shown to activate NADPH-dependent oxidase activity, leading to oxidative stress in human keratinocytes (24). Similarly, in the rat SLOS model, elevated 7-DHC and formation of lipid peroxides lead to retinal degeneration (22, 25). Although there is no direct correlation between plasma levels of 7-DHC and the severity of SLOS (26), it is not known if this correlation is present in specific tissues, especially the nervous system. Brain cholesterol biosynthesis is independent from whole-body cholesterol biosynthesis (27); different tissues may accumulate 7-DHC to different degrees and may metabolize 7-DHC or its derivatives differently. In some reported therapeutic studies of SLOS, cholesterol supplementation leads to no significant symptomatic improvement in SLOS patients (28–31). Thus, it is possible that 7-DHC accumulation within the nervous system, rather than cholesterol deficiency, may be critical for development of the nervous system pathophysiology associated with SLOS.

The observation that 7-DHC is such a reactive compound toward free radical reaction with molecular oxygen, producing a complex oxysterol mixture (32), coupled with the fact that it plays a prominent role in cholesterol biosynthesis and in SLOS, stimulated us to consider the biological activities of 7-DHC oxysterols in greater detail. The notion that 7-DHC oxysterols may be of interest was further supported by the fact that cholesterol-derived oxysterols have been the focus of many recent studies because of their interesting activities (23, 33–38). By analogy, it seems reasonable to suggest that 7-DHC oxysterols will have interesting activities, some of which may be associated with the pathophysiology of SLOS.

To test the functional effects of 7-DHC oxysterols on neuronal function, we: 1) oxidized 7-DHC *in vitro*, 2) isolated and purified individual oxysterols, 3) analyzed Dhcr7-deficient Neuro2a cells for the presence of oxysterols, 4) tested the effects of 7-DHC-derived oxysterols on cell viability, cell proliferation, growth, and gene expression, and 5) correlated oxysterol structure with biological activity. We report here the results of those studies and discuss the significance of these findings for SLOS.

MATERIALS AND METHODS

Materials

The initiator 2,2'-azobis(4-methoxy-2,4-dimethylvaleronitrile) was purchased from Wako Chemicals, dried under vacuum, and then stored at -40°C . 7-DHC (>98%) and Rose Bengal (95%) were purchased from Sigma-Aldrich Co. and were used without further purification. Benzene (HPLC grade) was passed through a column of neutral alumina and stored over molecular sieves. Hexanes, ethyl acetate, methylene chloride, and methanol (all

99.9%) were purchased from Thermo Fisher Scientific Inc. 7-Ketocholesterol was prepared by a known procedure (39).

Cell cultures

The neuroblastoma cell line Neuro2a was purchased from the American Type Culture Collection (Rockville, MD). Dhcr7-deficient and nonsilencing Neuro2a cells were generated as described previously (40). Dhcr7-deficient cells express short hairpin (sh) RNA that downregulates the Dhcr7 enzyme and leads to accumulation of 7-DHC when the cells are grown in lipid-deficient serum. Nonsilencing Neuro2a cells express nonsilencing shRNA vector. All cell lines were maintained in DMEM supplemented with L-glutamine, 10% FBS (Thermo Scientific HyClone, Logan, UT), and penicillin/streptomycin at 37°C and 5% CO_2 . According to the vendor, the FBS contained cholesterol at concentrations of 32 mg/100 ml. This translates into a final cholesterol concentration of 32 $\mu\text{g}/\text{ml}$ in our culture medium. For experiments shown in Fig. 1, cells were cultured with medium containing 10% cholesterol-deficient serum (Thermo Scientific HyClone Lipid Reduced FBS). This FBS medium did not have detectable cholesterol levels. While Neuro2a cultures were maintained in DMEM with phenol red, the experimental data was obtained from cultures grown in phenol-free DMEM medium. Dhcr7-deficient and control (transfected with nonsilencing shRNA) cells were grown in the presence of puromycin (40).

Lipid extraction, separation, and HPLC-MS/MS analyses of Neuro2a cells

Control and Dhcr7-deficient Neuro2a cultures were generated as discussed above and as previously reported (40). Cell pellets were collected after the cultures were grown for 5 days in lipid-deficient medium. Cell pellets were homogenized in Folch solution (5 ml, chloroform-methanol = 2/1, containing 0.001 M butylated hydroxytoluene and PPh_3) by vortexing and sonication for 20 s. A NaCl aqueous solution (0.9%, 1 ml) was then added, and the resulting mixture was vortexed for 1 min and centrifuged for 5 min. The lower organic phase was recovered, dried under nitrogen, redissolved in methylene chloride, and subject to separation with $\text{NH}_2\text{-SPE}$ [500 mg; the column was conditioned with 4 ml of hexanes, and the neutral lipids containing oxysterols were eluted with 4 ml of chloroform-isopropanol (2/1)]. The eluted fractions were then dried under nitrogen and reconstituted in methylene chloride (400 μl) for HPLC-MS/MS analyses. The analyses were carried out similarly to the method described previously (32). The HPLC conditions were: silica, 4.6 mm \times 25 cm column, 5 μm , 1.0 ml/min; elution solvent: 10% 2-propanol in hexanes. For MS, selective reaction monitoring was employed to monitor the dehydration process of the ion $[\text{M}+\text{H}-\text{H}_2\text{O}]^+$ in the MS. Thus, for oxysterols with a molecular weight of $[\text{7-DHC}+2\text{O}]$, dehydration of m/z 399 to 381 was monitored. For $[\text{7-DHC}+3\text{O}]$, m/z 415 to 397 was monitored. In this way, masses that correspond to 7-DHC plus 1, 2, 3, and 4 oxygen atoms can be monitored. Only the $[\text{7-DHC}+2\text{O}]$ and $[\text{7-DHC}+3\text{O}]$ masses showed major differences between control and Dhcr7-deficient cells, which are shown in Fig. 1 in the text. 25-Hydroxycholesterol was added to each sample as an external standard, which has a minor fragment, $[\text{M}-4\text{H}+\text{H}^+]$, with the same m/z of 399. As a result, 25-hydroxycholesterol was detected in the $[\text{7-DHC}+2\text{O}+\text{H}^+-\text{H}_2\text{O}]$ panel of Fig. 1 with the retention of 4.69 min.

Immunocytochemistry

Neuro2a cells were plated in 24-well plates at a density of 5,000 cells/well. Twenty-four hours after plating, the cells were treated with oxysterols (concentrations shown in text) for 24, 48, or 72 h and incubated at 37°C with 5% CO_2 . After the appropriate time in

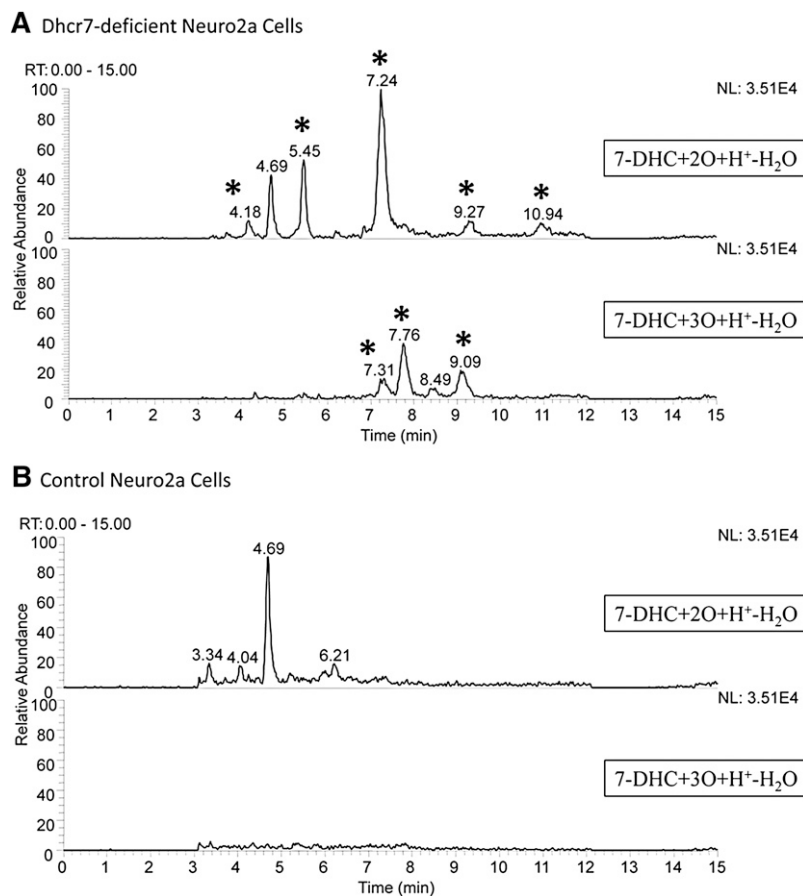


Fig. 1. 7-DHC oxysterols are present in Dhcr7-deficient Neuro2a cells. The chromatogram in panel A shows the oxysterol profile of Dhcr7-deficient Neuro2a cells. New peaks relative to control (B) are marked with an asterisk. The peak at RT = 4.69 min represents a minor MS fragment from the external standard 25-hydroxycholesterol.

the culture, the cells were washed with PBS and fixed for 15 min at room temperature in 4% paraformaldehyde. Following washing with PBS, the cells were incubated for 30 min in the blocking buffer (10% fetal bovine serum plus 0.1% saponin in PBS) at room temperature. Primary antibodies, anti-p75 (Promega), and Tu20 (Abcam) were diluted in blocking buffer 1:1,000 and incubated overnight at +4°C. After several washes in PBS, secondary antibody, anti-rabbit Cy3 (Sigma), was used at 1:2,000 for 1 h at room temperature. The cells were washed with PBS, a droplet of Fluoromount was added, and they were then coverslipped and analyzed on the Zeiss AXIO Observer.Z1 inverted microscope equipped with a Hamamatsu Digital Camera C10600 Orca R². Images were acquired using AxioVision Rel. 4.7 program. The objective lenses were Zeiss EC Plan-NEOFLUAR 10×/0.3 Ph1 (420341-9911) and Zeiss LD Plan-NEOFLUAR 20×/0.4 Ph2 Korr (∞ /0-1,5).

Total RNA isolation and quantitative PCR

The detailed description of total RNA isolation, quantitative PCR (qPCR), and primer sequences used in the current study were published recently (40, 41). The Ki67 primers used in the SYBR qPCR assay were: forward: actgcagcagatggaactagg, reverse: agaacagtagcgtgatgttgg. These primers were optimized and found to have a slope of -3.1 with $R = 0.99$.

Preparation of 7-DHC-derived oxysterols

Pure oxysterols 1–7 and 10 were isolated from 7-DHC free radical oxidation mixture as described previously (32). 7-DHC

photooxidation products 13–15 were prepared as reported (42, 43).

HPLC fractionation of 7-DHC oxysterols

Because the 7-DHC oxysterol mixture contains over a dozen compounds, we designed experiments to determine the activity of individual fractions collected from HPLC, aiming to find the most potent peaks. The 7-DHC oxidation product mixtures were obtained as reported previously (32). Briefly, 7-DHC (0.13 M) in benzene was oxidized under an atmosphere of O₂ at 37°C for 28 h with the radical initiator 2,2'-azobis(4-methoxy-2,4-dimethylvaleronitrile) (1 mol%), and the resulting reaction mixture was stored at -80°C until HPLC separation. The primary 7-DHC-oxidation mixture (0.11 M, 100 μl) was subject to separation by normal phase HPLC-UV (25 cm \times 10 mm, 5 μSi ; elution solvent: 10% 2-propanol in hexanes, flow rate: 4.0 ml/min, monitoring wavelengths: 210 and 246 nm) over a 40 min period. One minute fractions were collected beginning at the 3rd min until the 39th min. One milliliter of each collected fraction was saved for MS analysis. Half of this 1 ml was analyzed directly by HPLC-MS, and the other half was reduced by PPh₃ (0.1 M, 10 μl) before being analyzed by HPLC-MS. HPLC-MS analyses were carried out as previously reported (32). Peaks containing 1, 2a, 2b(OOH), 2b, 2b(OOH), 3, and 4 were identified by comparing with the retention time and mass spectra of the corresponding standards. The remaining 3 ml was dried under N₂ and used for cell viability tests.

The same procedure was applied to separation and collection of 7-DHC oxidation products (0.11 M, 100 μ l) reduced with an excess amount of P(OMe)₃. Similarly, 1 ml of each fraction was directly used for HPLC-MS analysis and 3 ml was used for cell viability tests.

A parallel HPLC-UV separation of 7-DHC oxidation products reduced with P(OMe)₃ was carried out to collect peaks eluting at 6.9, 7.9, 8.9, 9.2, 10.9, 11.9, 12.5, 13.0, and 15.5 min. ¹HNMR analysis on the collected peaks confirmed the peaks containing compounds **1**, **2a**, **2b**, **3**, and **4**, which is consistent with the HPLC-MS analysis.

The correlation between HPLC fractions and their effects on cell viability is shown in supplementary Fig. IIA, B.

In the chromatogram of the primary oxysterol mixture, the majority of bioactive compounds elute in the first 15 HPLC fractions. Among those, fractions 6, 7, 10, 11, and 12 contain the compounds most toxic to Neuro2a cells. In contrast, in the chromatogram of the reduced product mixture, fractions 6 and 7 are much less toxic compared with the comparable primary oxysterol fractions. The compound **2a**(OOH) was found to elute in fraction 6 of the primary product mixture and **2b**(OOH) elutes in fraction 7 (supplementary Fig. IIA). This suggests that the most toxic components in fractions 6 and 7 of the primary oxysterol product mixture are **2b**(OOH) and **2a**(OOH). Cell viability tests on purified compounds are consistent with this observation.

RESULTS

7-DHC oxysterols are present in Dhcr7-deficient Neuro2a cells

We hypothesized that oxysterols will be present in biological samples under normal metabolic conditions if 7-DHC is present at high levels because of the high oxidizability of this sterol. To test this hypothesis, we analyzed a cellular model for SLOS, Dhcr7-deficient Neuro2a cells (40). Neuro2a have a high endogenous level of the Dhcr7 enzyme and Dhcr7-deficient cells express shRNA that downregulates Dhcr7 and leads to accumulation of 7-DHC when the cells are grown in lipid-deficient medium (40). Dhcr7-deficient and nonsilenced cells were grown for 5 days in lipid-deficient medium and collected for HPLC-MS analysis. A representative chromatogram is shown in Fig. 1. A number of peaks that have *m/z* expected for 7-DHC oxysterols were found in the chromatogram of Dhcr7-deficient cells, whereas these compounds were not detected in the nonsilenced Neuro2a cells. The peak in the chromatogram at RT = 7.24 min was tentatively assigned as compound **10**, 3 β ,5 α -dihydroxycholesta-7-en-6-one, based on the exact retention time and mass spectrum compared with a standard isolated from 7-DHC oxidation product mixture (vide infra, also see Fig. 3) (32). Studies that confirm the presence of compound **10** and the structure elucidation of other compounds present in SLOS cell models are ongoing and will be reported in due course.

7-DHC oxysterol mixtures reduce Neuro2a cell viability in a dose- and time-dependent manner

Free radical oxidation of 7-DHC produces a complex primary oxysterol product mixture that contains hydroperoxides, cyclic peroxides, epoxides, and alcohols (32). It seems likely that this primary product mixture, if formed

in human cells and tissues, will be subject to metabolic detoxification (44). Indeed, there are a number of enzymes that serve to combat oxidative stress by the reduction of hydroperoxide functional groups, -OOH \rightarrow -OH (45, 46). We therefore developed methods to reduce hydroperoxide functionality in the primary 7-DHC oxysterol product mixture by a mild reducing agent that reduces hydroperoxides without modifying other functional groups.

Peroxidation of 7-DHC was carried out in solution as described previously (32), and the mixture of 7-DHC-derived oxysterols formed, which we identify hereafter as the primary oxysterol mixture (or the primary oxysterols), was added to cell cultures to determine their effect on cell survival. The 7-DHC-derived oxysterol mixture that was reduced, which we identify hereafter as the reduced oxysterol mixture, was also assayed for cytotoxicity. For these experiments, we used Neuro2a neuroblastoma cells that were treated with several concentrations (0–100 μ M) of the 7-DHC oxysterol mixtures for different periods of time (24–72 h) (Fig. 2, supplementary Fig. I). Cell viability was significantly reduced in a dose- and time-dependent manner for treatments with both the primary and reduced oxysterol mixtures. The reduced 7-DHC oxysterol mixture is more toxic than the primary mixture based on comparable effects of the primary mixture at 50 μ M and the effects of the reduced mixture at 25 μ M, suggesting that the toxicity of the mixture is not due to a general lipid hydroperoxide effect but is more intimately associated with the oxysterol nucleus structure. For comparison, 7-ketocholesterol and 7 β -hydroxycholesterol derived from cholesterol peroxidation trigger cell death, activate inflammation, and modulate lipid homeostasis, and their toxicities range from 30–100 μ M in monocytic cells to 10–100 nM in hippocampal neurons (35, 47, 48).

7-DHC-derived cyclic peroxides are the most toxic of all of the isolated 7-DHC oxysterols

Cell viability tests were carried out on Neuro2a cells with all fractions collected from an HPLC separation of the primary and reduced 7-DHC oxysterol mixtures. We conclude from these studies that all of the major potent compounds in the mixtures have known chemical structures that were previously assigned (32) (supplementary Fig. II). Subsequently, the Neuro2a cells were exposed to different concentrations of the individual purified 7-DHC-derived oxysterols, and the cytotoxicity of the 7-DHC oxysterol mixture was compared in each case to the activity of individual compounds. Compounds assayed in this way were the epoxy alcohols **1**, **6a**, and **6b**, the cyclic peroxides **2a**, **2b**, **3**, and **7**, the dienol **4**, trienol **5**, and tetraols **12a** and **12b**. In addition, three 7-DHC photo-oxidation products and 7-ketocholesterol were examined for cytotoxicity (Fig. 3, supplementary Fig. III).

Epoxy alcohol **1** and compound **7** do not affect apparent cell viability, whereas all other compounds decrease cell viability more than the 7-DHC oxysterol mixture. For most compounds, a concentration of 25 μ M reduces cell viability by 50% or more. The most toxic compounds are

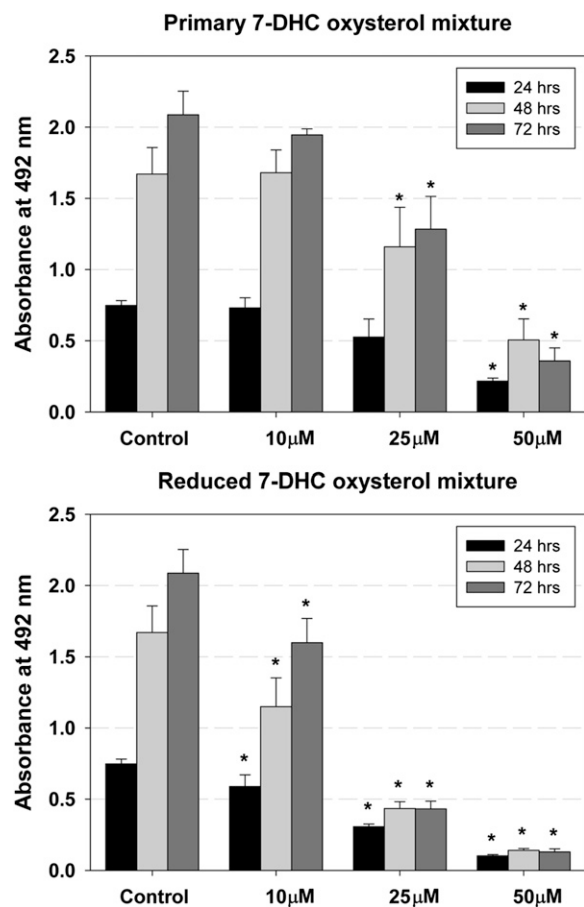


Fig. 2. Primary and reduced 7-DHC oxysterol mixtures reduce cell viability in a dose- and time-dependent manner. The *x*-axis shows different concentrations of oxysterol mixture, the *y*-axis shows absorbance at 492 nm, and different colors of the bars show different time points. Under control conditions, the number of cultured cells increases over the 72 h time period. Different concentrations of the 7-DHC oxysterol mixture have specific effects on cell survival; whereas treatment with 10 μ M concentration of primary mixture does not differ from control, 10 μ M of the reduced mixture significantly reduces the cell number. The error bars show SD and the stars show significant change ($P < 0.01$).

endoperoxides **2a**, **2b**, and **3**, which all affect cell viability at 5 μ M concentrations. While these compounds all contain an endoperoxide functional group linking carbons 5 and 9 on the steroid ring B, compound **7** has a similar endoperoxide but has little, if any, cytotoxicity. Clearly, these cytotoxicity effects depend on subtle structural differences, and generalizations about structure-activity should be advanced with some caution at this time.

7-DHC-derived oxysterols reduce proliferation of Neuro2a cells

Neuro2a cells are a rapidly proliferating neuroblastoma cell line. The reduced cell viability in these cells when exposed to oxysterols could be the result of reduced proliferation, cell death, or both. Ki67 is a cell cycle-related nuclear protein expressed by proliferating cells in all phases of the active cell cycle, and it is routinely used as a marker of cell proliferation (49). qPCR for the expression level of *Ki67* mRNA shows that the

reduced 7-DHC oxysterol mixture downregulates *Ki67* expression by about 3.2-fold and compound **10** downregulates *Ki67* expression even more than the oxysterol mixture (4.3-fold) (Fig. 4).

7-DHC-derived oxysterols induce differentiation of Neuro2a cells

Compared with control Neuro2a cells that are amoeboid irregularly shaped cells, we noticed that 7-DHC-oxysterol-treated cells show significant morphological changes. The concentration of the 7-DHC oxysterol mixture that led to a 50% reduction in cell survival was used to treat Neuro2a cultures for 24–72 h, and the morphological changes of the cells were analyzed by the use of Tu20 and p75 antibodies. Tu20 recognizes neuron-specific β III tubulin and it is used as a differentiation marker (50). The P75 antibody recognizes neurotrophic receptor p75 that is expressed at high levels in Neuro2a cells and stains both cell bodies and processes (41, 51). Microscopic examination showed that in the presence of the 7-DHC oxysterol mixture, Neuro2a cells develop long processes (Fig. 5). These changes are visible within hours of treatment and persist in culture for at least 72 h. The differentiation effect is observable even with lower concentrations of the 7-DHC oxysterol mixture, but it is not as dramatic as shown in Fig. 5. Both primary and reduced oxysterol mixtures lead to similar morphological changes. The same morphology is observed with both Tu20 and p75 antibodies (supplementary Fig. IV). Undifferentiated Neuro2a cells express very low levels of β III tubulin, while they express significantly more p75. Therefore, under control conditions, the staining of cell bodies is more prominent with the anti-p75 antibody (supplementary Fig. IV). Differentiated Neuro2a cells upregulate expression of β III tubulin, and both cell bodies and processes are very brightly stained with Tu20 antibody.

Transcriptome changes that are observed in Dhcr7-deficient Neuro2a cells are also observed in control Neuro2a cells when treated with 7-DHC oxysterols

We reported previously that Dhcr7 deficiency in Neuro2a cells leads to transcriptome changes (40) and to better understand the molecular consequences of oxysterol treatment, we analyzed treated and control cells by qPCR at 24 h (Fig. 4) and 48 h (supplementary Fig. V) after treatment. We chose to analyze the expression level of the same transcripts that we found altered in Dhcr7-deficient Neuro2a cells (40). These include *Adam 19*, *Egr1*, *20Rik*, *Prr13*, *Snag1*, *Snx6*, and lipid biosynthesis genes (*FASN*, *SREBP2*, *SCAP*, *SIP*, and *SQSI*). We found that 7-DHC oxysterols indeed induce changes in the same set of genes in control cells as those that were identified in Dhcr7-deficient cells. With the exception of the *Snx6* transcript that is not affected by oxysterols, the treated cells generally show more pronounced effects than those observed in Dhcr7-deficient cells; the magnitude of change in oxysterol-treated cells is on average more than 1 $\Delta\Delta$ Ct (2-fold) compared with less than 1 $\Delta\Delta$ Ct in Dhcr7-deficient cells.

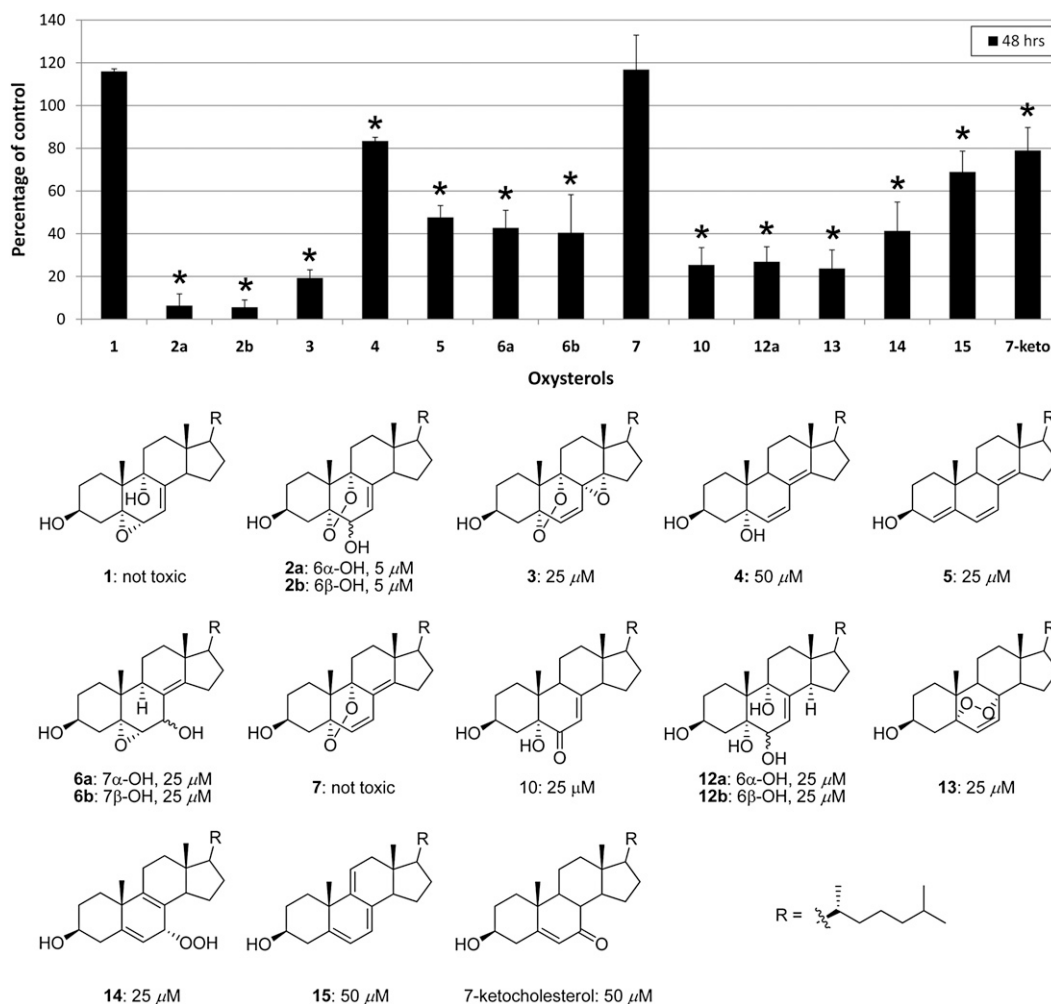


Fig. 3. Individual 7-DHC oxysterols show toxicity equal to or greater than the oxysterol mixture, correlation of structures with cellular effects. A: Neuro2a cells were treated with purified oxysterols (25 μ M), and cell survival was analyzed 48 h later. At this concentration, a majority of compounds reduces cell viability to $<50\%$ ($P < 0.001$, marked with star). Compounds 1 and 7 are not toxic and compound 4 reduces cell survival by 20% ($P < 0.01$). B: Chemical structures of oxysterols. Compounds 1–12 are formed from free radical oxidation of 7-DHC. Compounds 13–15 are formed from photo-oxidation of 7-DHC. The number below each compound shows the oxysterol concentration that leads to reduction in cell survival to $\leq 50\%$ at 48 h after the treatment.

Both primary and reduced 7-DHC oxysterols trigger expression changes similar to those observed in *Dhcr7*-deficient cells. However, compound 10 shows a slightly different gene expression profile. Whereas compound 10 regulates expression of *Ki67*, *Prr13*, *Adam19*, *Egr1*, and *Snag1*, it does not affect the lipid biosynthesis enzymes except the *Dhcr7* transcript. The observed changes in lipid transcripts induced with primary and reduced 7-DHC oxysterol treatment are in agreement with published reports on the ability of cholesterol-derived oxysterols modulating lipid biosynthesis (33).

DISCUSSION

The products of fatty acid and cholesterol peroxidation may serve as biomarkers of oxidative stress, but they may also exert significant biological activities and play important roles in cell signaling and gene induction (52,

53). Based on the studies reported here, we conclude that the majority of the oxysterols formed from peroxidation of 7-DHC are bioactive and strongly affect cell viability. Indeed, the oxysterol mixture formed from peroxidation of 7-DHC strongly reduces cell proliferation in Neuro2a cells and leads to induction of cell differentiation.

The set of 7-DHC-derived products is remarkably complex compared with the products that are normally observed from peroxidation of cholesterol. Cholesterol is a mono-alkene that, upon peroxidation, gives primarily oxo-, hydroxyl-, and hydroperoxyl-substituted derivatives at C-7 of the sterol structure. 7-DHC, on the other hand, is a diene and this provides additional mechanistic options. A detailed reaction mechanism that involves abstraction of hydrogen atoms at C-9 and/or C14 of the sterol was presented recently to account for the formation of all of the isolated oxysterols (32).

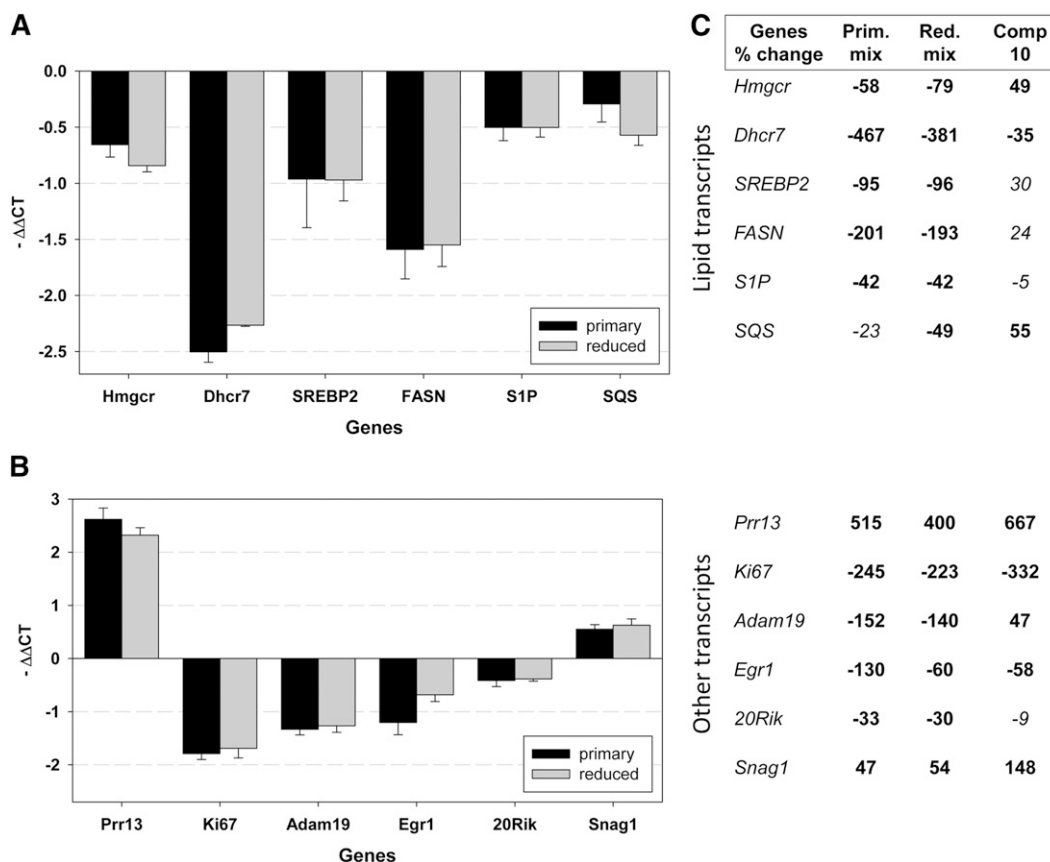


Fig. 4. Oxysterol treatment of control Neuro2a leads to gene expression changes. In the graphs A and B, the genes are plotted on the x-axis, and the y-axis denotes the average $-\Delta\Delta Ct$ that was calculated against Tbp1 as a normalizer. $P < 0.001$ for changes shown in bold and not significant for those in *italic*. A: Oxysterol treatment results in decreased expression of critical lipid biosynthesis genes that were also found altered in Dhcr7-deficient Neuro2a cells. The results are concordant for the primary (50 μM) and reduced (25 μM) mixtures. Compound 10 significantly affects the expression of Dhcr7 at both 24 and 48 h, but the effect on other lipid genes is not consistent and not significant. B: Oxysterol treatment results in gene expression changes similar to those identified in Dhcr7-deficient Neuro2a cells. Whereas Prr13, Egr1, and Snag1 showed consistent changes at both the 24 and 48 h time points, Adam19 and 20Rik were not changed at 48 h, suggesting transient change in the expression of these genes in response to oxysterol treatment. Compound 10 affects the expression of Ki67, Prr13, Egr1, and Snag1 similarly to primary and reduced mixtures. C: Summary of gene expression changes expressed as percentage of untreated cells. The table lists the genes and percentage of change. The changes are upregulation (positive value) and downregulation (negative value). For details of gene expression changes in Dhcr7-deficient cells, see Korade et al. (40).

Our studies show that several oxysterols are present in the SLOS Neuro2a cell models, and these compounds are not found in control Neuro2a cells (Fig. 1). One of these oxysterols is tentatively assigned as compound **10** on the basis of identical mass spectra and retention times compared with the isolated standard. Compound **10** is a constituent of the product mixture formed from the free radical oxidation of 7-DHC, and this is highly suggestive that peroxidation of 7-DHC is linked to cellular changes in SLOS.

Compound **10** as well as oxysterol mixture induce transcriptome changes in the cholesterol and lipid biosynthesis pathways. However, compound **10** shows slightly different changes than those found for the 7-DHC oxysterol mixture. It is not surprising that the individual 7-DHC oxysterols would show differential effects on induction of specific genes, because they most likely act as specific ligands for different liver X receptors (LXRs) or other tran-

scription factors (54–56). The most potent endogenous ligands for LXRs are 24S-hydroxycholesterol, 24S,25-epoxycholesterol, 24-oxocholesterol, 27-hydroxycholesterol, and desmosterol (57–60). The drastic differences between the core structures of 7-DHC-derived oxysterols and the structures of the classic ligands for LXRs may provide much needed guidance for the study of structure-activity relationships of nuclear receptor ligands (57). Indeed, oxysterols are ligands not only for LXRs and retinoid X receptors but also for other nuclear receptors (61). In addition, there is a very large family of oxysterol-binding proteins, and different oxysterols may work in concert with specific binding proteins (62). This is in agreement with our finding that the cellular transcriptome changes triggered by 7-DHC-derived oxysterols in control Neuro2a cells overlap with the changes observed in Dhcr7-deficient cells, suggesting a role for oxysterols not only in lipid biosynthesis but also in other aspects of cellular metabolism.

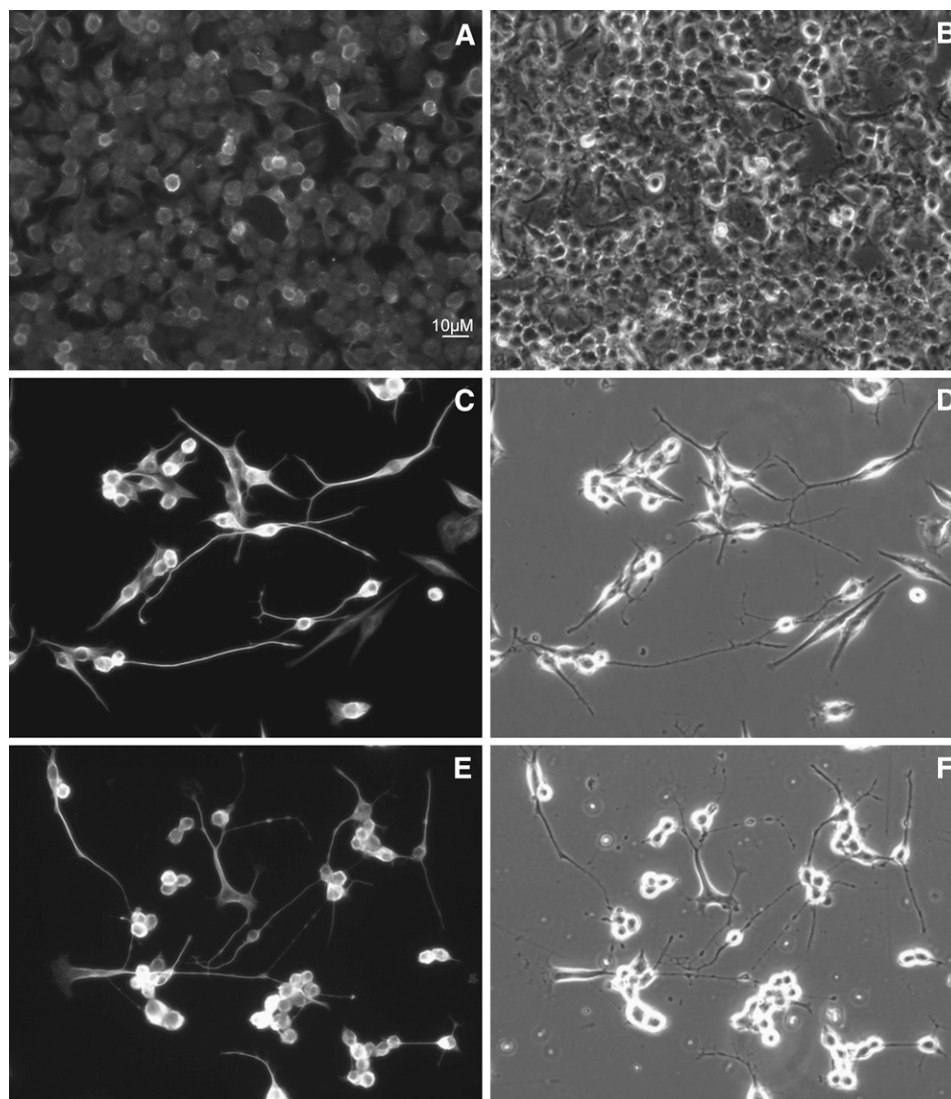


Fig. 5. Both primary and reduced 7-DHC oxysterol mixtures induce differentiation of Neuro2a cells. After 48 h of oxysterol treatment, cells were fixed and processed for immunocytochemistry using Tu20 (A, C, E) antibody. Panels on the left show Cy3 fluorescence and the panels on the right show phase contrast of the same field. A and B are control, C and D are treated with 50 μ M primary 7-DHC oxysterol mixture, and E and F are treated with 25 μ M reduced mixture.

Indeed, our studies are in agreement with a recent proposal by Fliesler (63) suggesting that SLOS is not only an imbalance of cholesterol and 7-DHC caused by defects in *Dhcr7*, but it also involves secondary defects in nonsterol metabolic pathways and additional biochemical changes (63). Low levels of cholesterol are present in several disorders arising from defects in different enzymes in the cholesterol biosynthesis pathway (CDPX2, lathosterolosis, desmosterolosis) (18, 64). Because the phenotype is specific for different disorders, it is very likely that in addition to low levels of cholesterol there are other contributing factors, including the accumulation of sterol intermediates. This is supported by recent studies that analyzed *Insig* double KO mice (65–67). *Insig* proteins regulate cholesterol biosynthesis through modulating the activities of *Hmgcr* and *Scap* (68). In these mice, accumulation of cholesterol intermediates in the presence of cholesterol leads to cleft palate (65) or hair growth defects (67). Be-

cause the cholesterol precursors and their oxidized forms may be bioactive and potentially toxic, careful isolation and characterization of specific sterols and oxysterols in these KO mice may prove to be of interest. Studies directed toward identification of other 7-DHC-derived oxysterols found in SLOS cell models and assessment of their biological activities are ongoing in our laboratories and will be reported in due course. The examination of human SLOS fibroblasts and knockout rodents will also be carried out to explore the role of 7-DHC oxysterols in these systems.

What is the significance of our findings for SLOS? In SLOS, 7-DHC accumulates in tissue and fluids. Whereas control populations show plasma cholesterol levels of \sim 180 mg/dl and 7-DHC of \sim 0.005–0.05 mg/dl, SLOS patients can have plasma cholesterol levels of \sim 85 mg/dl or lower and 7-DHC levels as high as \sim 25 mg/dl (20, 28). A rough calculation of the kinetics of oxysterol product

formation predicts that SLOS tissue would have roughly 27 times higher levels of oxysterols (including those derived both from cholesterol and 7-DHC) than control tissue, given comparable levels of radical initiation and termination. But the accumulation of 7-DHC-derived oxysterols may be dependent on several factors. First, levels could be higher in tissues exposed to high oxygen tension (e.g., lung, retina) or in tissues that are relatively deficient in endogenous antioxidants. For example, a cholesterol-derived oxysterol that is structurally analogous to compound **10** has been reported to be present in ozone-exposed lung lavage and in a human bronchial epithelial cell line, and this oxysterol appears to be toxic at micromolar concentrations (69). Light has been reported to exacerbate retina degeneration in a rat model of SLOS and this observation could well be due to accelerated free radical oxidation of 7-DHC (22, 70). In addition, the formation and accumulation of 7-DHC oxysterols might be modified by enzymatic transformations, and therefore different tissues may show specific 7-DHC-derived oxysterol profiles. Oxysterol levels could also be tissue and fluid dependent, because 7-DHC concentrations differ in plasma, brain, and liver in humans and rodent models (11, 20, 28, 71–73).

Targeted lipidomic analyses of the mouse embryonic brain showed the presence of endogenous cholesterol-derived oxysterols of enzymatic and nonenzymatic origin (74). Therefore, it is likely that 7-DHC would serve as a source of oxysterols in the developing and adult brain. Considering the potent biological effects of 7-DHC-derived oxysterols, it is probable that these accumulated oxysterols would influence normal brain development. Because hippocampal neurons are more sensitive than monocytic cells to 7-ketocholesterol (47, 48), it is likely that primary neurons will be more sensitive to 7-DHC-derived oxysterols than Neuro2a, a neuroblastoma cell line. In addition, the accumulation and metabolism of oxysterols and the sensitivity to oxysterols may differ between neuronal and glial cells. Even small changes in proliferation rate of neuronal progenitors induced by oxysterols as well as their effect on differentiation of neuronal precursors into specific types of neurons would greatly influence brain development. For example, in the mouse SLOS model, there is an increase in number of serotonergic neurons and fibers and changes in the fiber tract formation (agenesis of corpus callosum and agenesis of hippocampal commissure) (75). Future studies will show if some of these changes are the result of 7-DHC oxysterol accumulation in the nervous system of the SLOS KO mice.

Gene expression changes due to deficiency of Dhcr7 reductase were examined previously in both in vivo and in vitro models (40, 75). Waage-Baudet's (75) study analyzed gene expression changes in embryonic hindbrain of Dhcr7-deficient mice, and Korade et al. (40) analyzed gene expression changes in Dhcr7-deficient Neuro2a cells. Despite the many differences in methodologies used in these two studies (starting material, experimental design, data mining, microarray platform), there is a concordance in the results showing expression changes in cholesterol synthe-

sis, sterol metabolism/transport, and fatty acid synthesis. Based on the identification of overlapping gene expression changes in Dhcr7-deficient and 7-DHC oxysterol-treated Neuro2a cells, we hypothesize that the pathophysiological findings in the mouse SLOS model and SLOS patients might be due to accumulated 7-DHC oxysterols. Should this prove to be the case, it would potentially change the paradigm for SLOS therapy, shifting the focus to the identification of therapeutic agents that prevent the formation (or neutralization) of the most toxic 7-DHC-derived oxysterols. ■■

Z.K. appreciates support from the Vanderbilt Kennedy Center for Research on Human Development. Special thanks to Drs. Aaron Bowman for the use of the Zeiss inverted microscope and Karoly Mirnics for the use of the tissue culture facility and ABI system. We also thank Amy Millsap for collecting HPLC fractions and Khine Lwin for designing Ki67 primers.

REFERENCES

- Porter, N. A. 1986. Mechanisms for the autoxidation of polyunsaturated lipids. *Acc. Chem. Res.* **19**: 262–270.
- Porter, N. A., S. E. Caldwell, and K. A. Mills. 1995. Mechanisms of free radical oxidation of unsaturated lipids. *Lipids.* **30**: 277–290.
- Yin, H., and N. A. Porter. 2005. New insights regarding the autoxidation of polyunsaturated fatty acids. *Antioxid. Redox Signal.* **7**: 170–184.
- Porter, N. A., M. O. Funk, D. W. Gilmore, R. Isaac, and J. Nixon. 1976. The formation of cyclic peroxides from unsaturated hydroperoxides: models for prostaglandin biosynthesis. *J. Am. Chem. Soc.* **98**: 6000–6005.
- Porter, N. A., B. A. Weber, H. Weenen, and J. A. Khan. 1980. Autoxidation of polyunsaturated lipids. Factors controlling the stereochemistry of product hydroperoxides. *J. Am. Chem. Soc.* **102**: 5597–5601.
- Pratt, D. A., J. H. Mills, and N. A. Porter. 2003. Theoretical calculations of carbon-oxygen bond dissociation enthalpies of peroxy radicals formed in the autoxidation of lipids. *J. Am. Chem. Soc.* **125**: 5801–5810.
- Xu, L., T. A. Davis, and N. A. Porter. 2009. Rate constants for peroxidation of polyunsaturated fatty acids and sterols in solution and in liposomes. *J. Am. Chem. Soc.* **131**: 13037–13044.
- Korcek, S., J. H. B. Chenier, J. A. Howard, and K. U. Ingold. 1972. Absolute rate constants for hydrocarbon autoxidation. 21. Activation-energies for propagation and correlation of propagation rate constants with carbon-hydrogen bond strengths. *Can. J. Chem.* **50**: 2285–2297.
- Smith, D. W., L. Lemli, and J. M. Opitz. 1964. A newly recognized syndrome of multiple congenital anomalies. *J. Pediatr.* **64**: 210–217.
- Tint, G. S., M. Irons, E. R. Elias, A. K. Batta, R. Frieden, T. S. Chen, and G. Salen. 1994. Defective cholesterol biosynthesis associated with the Smith-Lemli-Opitz syndrome. *N. Engl. J. Med.* **330**: 107–113.
- Tint, G. S., M. Sella, R. Hughes-Benzie, A. K. Batta, S. Shefer, D. Genest, M. Irons, E. Elias, and G. Salen. 1995. Markedly increased tissue concentrations of 7-dehydrocholesterol combined with low levels of cholesterol are characteristic of the Smith-Lemli-Opitz syndrome. *J. Lipid Res.* **36**: 89–95.
- Jira, P. E., R. J. Wanders, J. A. Smeitink, J. De Jong, R. A. Wevers, W. Oostheim, J. H. Tuerlings, R. C. Hennekam, R. C. Sengers, and H. R. Waterham. 2001. Novel mutations in the 7-dehydrocholesterol reductase gene of 13 patients with Smith-Lemli-Opitz syndrome. *Ann. Hum. Genet.* **65**: 229–236.
- Krakowiak, P. A., N. A. Nwokoro, C. A. Wassif, K. P. Battaile, M. J. Nowaczyk, W. E. Connor, C. Maslen, R. D. Steiner, and F. D. Porter. 2000. Mutation analysis and description of sixteen RSH/Smith-Lemli-Opitz syndrome patients: polymerase chain reaction-based assays to simplify genotyping. *Am. J. Med. Genet.* **94**: 214–227.

14. Salen, G., S. Shefer, A. K. Batta, G. S. Tint, G. Xu, A. Honda, M. Irons, and E. R. Elias. 1996. Abnormal cholesterol biosynthesis in the Smith-Lemli-Opitz syndrome. *J. Lipid Res.* **37**: 1169–1180.
15. Witsch-Baumgartner, M., J. Löffler, and G. Utermann. 2001. Mutations in the human DHCR7 gene. *Hum. Mutat.* **17**: 172–182.
16. Honda, A., G. S. Tint, G. Salen, A. K. Batta, T. S. Chen, and S. Shefer. 1995. Defective conversion of 7-dehydrocholesterol to cholesterol in cultured skin fibroblasts from Smith-Lemli-Opitz syndrome homozygotes. *J. Lipid Res.* **36**: 1595–1601.
17. Kelley, R. I., and R. C. Hennekam. 2000. The Smith-Lemli-Opitz syndrome. *J. Med. Genet.* **37**: 321–335.
18. Porter, F. D. 2003. Human malformation syndromes due to inborn errors of cholesterol synthesis. *Curr. Opin. Pediatr.* **15**: 607–613.
19. Sikora, D. M., K. Pettit-Kekel, J. Penfield, L. S. Merckens, and R. D. Steiner. 2006. The near universal presence of autism spectrum disorders in children with Smith-Lemli-Opitz syndrome. *Am. J. Med. Genet. A.* **140**: 1511–1518.
20. Bukelis, I., F. D. Porter, A. W. Zimmerman, and E. Tierney. 2007. Smith-Lemli-Opitz syndrome and autism spectrum disorder. *Am. J. Psychiatry.* **164**: 1655–1661.
21. Gaoua, W., F. Chevy, C. Roux, and C. Wolf. 1999. Oxidized derivatives of 7-dehydrocholesterol induce growth retardation in cultured rat embryos: a model for antenatal growth retardation in the Smith-Lemli-Opitz syndrome. *J. Lipid Res.* **40**: 456–463.
22. Richards, M. J., B. A. Nagel, and S. J. Fliesler. 2006. Lipid hydroperoxide formation in the retina: correlation with retinal degeneration and light damage in a rat model of Smith-Lemli-Opitz syndrome. *Exp. Eye Res.* **82**: 538–541.
23. Schropfer, G. J., Jr. 2000. Oxysterols: modulators of cholesterol metabolism and other processes. *Physiol. Rev.* **80**: 361–554.
24. Valencia, A., A. Rajadurai, A. B. Carle, and I. E. Kochevar. 2006. 7-Dehydrocholesterol enhances ultraviolet A-induced oxidative stress in keratinocytes: roles of NADPH oxidase, mitochondria, and lipid rafts. *Free Radic. Biol. Med.* **41**: 1704–1718.
25. Lee, J. W., J. Sanchez, R. Riddick, J-D. Huang, S. J. Fliesler, and I. R. Rodriguez. 2009. Potentiation of visible light-induced photodamage in cultured RPE cells by treatment with AY9944, a 7-dehydrocholesterol reductase inhibitor. (Abstract #1843 in Annual Meeting Association for Research in Vision and Ophthalmology, Ft. Lauderdale, FL).
26. Tint, G. S., A. K. Batta, G. Xu, S. Shefer, A. Honda, M. Irons, E. R. Elias, and G. Salen. 1997. The Smith-Lemli-Opitz syndrome: a potentially fatal birth defect caused by a block in the last enzymatic step in cholesterol biosynthesis. *Subcell. Biochem.* **28**: 117–144.
27. Dietschy, J. M., and S. D. Turley. 2001. Cholesterol metabolism in the brain. *Curr. Opin. Lipidol.* **12**: 105–112.
28. Haas, D., S. F. Garbade, C. Vohwinkel, N. Muschol, F. K. Trefz, J. M. Penzien, J. Zschocke, G. F. Hoffmann, and P. Burgard. 2007. Effects of cholesterol and simvastatin treatment in patients with Smith-Lemli-Opitz syndrome (SLOS). *J. Inher. Metab. Dis.* **30**: 375–387.
29. Sikora, D. M., M. Ruggiero, K. Pettit-Kekel, L. S. Merckens, W. E. Connor, and R. D. Steiner. 2004. Cholesterol supplementation does not improve developmental progress in Smith-Lemli-Opitz syndrome. *J. Pediatr.* **144**: 783–791.
30. Starck, L., A. Lovgren-Sandblom, and I. Bjorkhem. 2002. Cholesterol treatment forever? The first Scandinavian trial of cholesterol supplementation in the cholesterol-synthesis defect Smith-Lemli-Opitz syndrome. *J. Intern. Med.* **252**: 314–321.
31. Tierney, E., S. K. Conley, H. Goodwin, and F. D. Porter. 2010. Analysis of short-term behavioral effects of dietary cholesterol supplementation in Smith-Lemli-Opitz syndrome. *Am. J. Med. Genet. A.* **152A**: 91–95.
32. Xu, L., Z. Korade, and N. A. Porter. 2010. Oxysterols from free radical chain oxidation of 7-dehydrocholesterol: product and mechanistic studies. *J. Am. Chem. Soc.* **132**: 2222–2232.
33. Brown, A. J., and W. Jessup. 2009. Oxysterols: Sources, cellular storage and metabolism, and new insights into their roles in cholesterol homeostasis. *Mol. Aspects Med.* **30**: 111–122.
34. Javitt, N. B. 2008. Oxysterols: novel biologic roles for the 21st century. *Steroids.* **73**: 149–157.
35. Lemaire-Ewing, S., C. Prunet, T. Montange, A. Vejux, A. Berthier, G. Bessedé, L. Corcos, P. Gambert, D. Neel, and G. Lizard. 2005. Comparison of the cytotoxic, pro-oxidant and pro-inflammatory characteristics of different oxysterols. *Cell Biol. Toxicol.* **21**: 97–114.
36. Smith, W. L., and R. C. Murphy. 2008. Oxidized lipids formed non-enzymatically by reactive oxygen species. *J. Biol. Chem.* **283**: 15513–15514.
37. Murphy, R. C., and K. M. Johnson. 2008. Cholesterol, reactive oxygen species, and the formation of biologically active mediators. *J. Biol. Chem.* **283**: 15521–15525.
38. Vejux, A., and G. Lizard. 2009. Cytotoxic effects of oxysterols associated with human diseases: Induction of cell death (apoptosis and/or oncosis), oxidative and inflammatory activities, and phospholipidosis. *Mol. Aspects Med.* **30**: 153–170.
39. Pearson, A., Y. Chen, G. Han, S. Hsu, and T. Ray. 1985. A new method for the oxidation of alkenes to enones: an efficient synthesis of delta-5-7-oxo steroids. *J. Chem. Soc. Perkins Trans. I.* 267–273.
40. Korade, Z., A. K. Kenworthy, and K. Mirmics. 2009. Molecular consequences of altered neuronal cholesterol biosynthesis. *J. Neurosci. Res.* **87**: 866–875.
41. Korade, Z., Z. Mi, C. Portugal, and N. F. Schor. 2007. Expression and p75 neurotrophin receptor dependence of cholesterol synthetic enzymes in adult mouse brain. *Neurobiol. Aging.* **28**: 1522–1531.
42. Albro, P. W., P. Bilski, J. T. Corbett, J. L. Schroeder, and C. F. Chignell. 1997. Photochemical reactions and phototoxicity of sterols: novel self-perpetuating mechanisms for lipid photooxidation. *Photochem. Photobiol.* **66**: 316–325.
43. Albro, P. W., J. T. Corbett, and J. L. Schroeder. 1994. Doubly allylic hydroperoxide formed in the reaction between sterol 5,7-dienes and singlet oxygen. *Photochem. Photobiol.* **60**: 310–315.
44. Bindoli, A., J. M. Fukuto, and H. J. Forman. 2008. Thiol chemistry in peroxidase catalysis and redox signaling. *Antioxid. Redox Signal.* **10**: 1549–1564.
45. Comhair, S. A., and S. C. Erzurum. 2005. The regulation and role of extracellular glutathione peroxidase. *Antioxid. Redox Signal.* **7**: 72–79.
46. Ursini, F., M. Maiorino, and C. Gregolin. 1985. The selenoenzyme phospholipid hydroperoxide glutathione peroxidase. *Biochim. Biophys. Acta.* **839**: 62–70.
47. Berthier, A., S. Lemaire-Ewing, C. Prunet, S. Monier, A. Athias, G. Bessedé, J. P. Pais de Barros, A. Laubriet, P. Gambert, G. Lizard, et al. 2004. Involvement of a calcium-dependent dephosphorylation of BAD associated with the localization of Trpc-1 within lipid rafts in 7-ketocholesterol-induced THP-1 cell apoptosis. *Cell Death Differ.* **11**: 897–905.
48. Nelson, T. J., and D. L. Alkon. 2005. Oxidation of cholesterol by amyloid precursor protein and beta-amyloid peptide. *J. Biol. Chem.* **280**: 7377–7387.
49. Gerdes, J., H. Lemke, H. Baisch, H. H. Wacker, U. Schwab, and H. Stein. 1984. Cell cycle analysis of a cell proliferation-associated human nuclear antigen defined by the monoclonal antibody Ki-67. *J. Immunol.* **133**: 1710–1715.
50. Theodorou, E., G. Dalembert, C. Heffelfinger, E. White, S. Weissman, L. Corcoran, and M. Snyder. 2009. A high throughput embryonic stem cell screen identifies Oct-2 as a bifunctional regulator of neuronal differentiation. *Genes Dev.* **23**: 575–588.
51. Chao, M. V. 1994. The p75 neurotrophin receptor. *J. Neurobiol.* **25**: 1373–1385.
52. Comporti, M., C. Signorini, B. Arezzini, D. Vecchio, B. Monaco, and C. Gardi. 2008. F2-isoprostanes are not just markers of oxidative stress. *Free Radic. Biol. Med.* **44**: 247–256.
53. van Reyk, D. M., A. J. Brown, L. M. Hult'en, R. T. Dean, and W. Jessup. 2006. Oxysterols in biological systems: sources, metabolism and pathophysiological relevance. *Redox Rep.* **11**: 255–262.
54. Wang, L., G. U. Schuster, K. Hulthenby, Q. Zhang, S. Andersson, and J. A. Gustafsson. 2002. Liver X receptors in the central nervous system: from lipid homeostasis to neuronal degeneration. *Proc. Natl. Acad. Sci. USA.* **99**: 13878–13883.
55. Edwards, P. A., M. A. Kennedy, and P. A. Mak. 2002. LXRs; oxysterol-activated nuclear receptors that regulate genes controlling lipid homeostasis. *Vascul. Pharmacol.* **38**: 249–256.
56. Zhao, C., and K. Dahlman-Wright. 2010. Liver X receptor in cholesterol metabolism. *J. Endocrinol.* **204**: 233–240.
57. Janowski, B. A., M. J. Grogan, S. A. Jones, G. B. Wisely, S. A. Kliewer, E. J. Corey, and D. J. Mangelsdorf. 1999. Structural requirements of ligands for the oxysterol liver X receptors LXRA and LXRbeta. *Proc. Natl. Acad. Sci. USA.* **96**: 266–271.
58. Janowski, B. A., P. J. Willy, T. R. Devi, J. R. Falck, and D. J. Mangelsdorf. 1996. An oxysterol signalling pathway mediated by the nuclear receptor LXR alpha. *Nature.* **383**: 728–731.
59. Lehmann, J. M., S. A. Kliewer, L. B. Moore, T. A. Smith-Oliver, B. B. Oliver, J. L. Su, S. S. Sundseth, D. A. Winegar, D. E. Blanchard, T. A. Spencer, et al. 1997. Activation of the nuclear receptor LXR by

- oxysterols defines a new hormone response pathway. *J. Biol. Chem.* **272**: 3137–3140.
60. Spencer, T. A., D. Li, J. S. Russel, J. L. Collins, R. K. Bledsoe, T. G. Consler, L. B. Moore, C. M. Galardi, D. D. McKee, J. T. Moore, et al. 2001. Pharmacophore analysis of the nuclear oxysterol receptor LXRalpha. *J. Med. Chem.* **44**: 886–897.
 61. Handschin, C., and U. A. Meyer. 2005. Regulatory network of lipid-sensing nuclear receptors: roles for CAR, PXR, LXR, and FXR. *Arch. Biochem. Biophys.* **433**: 387–396.
 62. Im, Y. J., S. Raychaudhuri, W. A. Prinz, and J. H. Hurley. 2005. Structural mechanism for sterol sensing and transport by OSBP-related proteins. *Nature*. **437**: 154–158.
 63. Fliesler, S. J. 2010. Retinal degeneration in a rat model of smith-lemli-opitz syndrome: thinking beyond cholesterol deficiency. *Adv. Exp. Med. Biol.* **664**: 481–489.
 64. Herman, G. E. 2003. Disorders of cholesterol biosynthesis: prototypic metabolic malformation syndromes. *Hum. Mol. Genet.* **12**: R75–R88.
 65. Engelking, L. J., B. M. Evers, J. A. Richardson, J. L. Goldstein, M. S. Brown, and G. Liang. 2006. Severe facial clefting in Insig-deficient mouse embryos caused by sterol accumulation and reversed by lovastatin. *J. Clin. Invest.* **116**: 2356–2365.
 66. Porter, F. D. 2006. Cholesterol precursors and facial clefting. *J. Clin. Invest.* **116**: 2322–2325.
 67. Evers, B. M., M. S. Farooqi, J. M. Shelton, J. A. Richardson, J. L. Goldstein, M. S. Brown, and G. Liang. 2010. Hair growth defects in Insig-deficient mice caused by cholesterol precursor accumulation and reversed by simvastatin. *J. Invest. Dermatol.* **130**: 1237–1248.
 68. Engelking, L. J., G. Liang, R. E. Hammer, K. Takaishi, H. Kuriyama, B. M. Evers, W. P. Li, J. D. Horton, J. L. Goldstein, and M. S. Brown. 2005. Schoenheimer effect explained—feedback regulation of cholesterol synthesis in mice mediated by Insig proteins. *J. Clin. Invest.* **115**: 2489–2498.
 69. Pulfer, M. K., and R. C. Murphy. 2004. Formation of biologically active oxysterols during ozonolysis of cholesterol present in lung surfactant. *J. Biol. Chem.* **279**: 26331–26338.
 70. Vaughan, D. K., N. S. Peachey, M. J. Richards, B. Buchan, and S. J. Fliesler. 2006. Light-induced exacerbation of retinal degeneration in a rat model of Smith-Lemli-Opitz syndrome. *Exp. Eye Res.* **82**: 496–504.
 71. Wassif, C. A., P. Zhu, L. Kratz, P. A. Krakowiak, K. P. Battaile, F. F. Weight, A. Grinberg, R. D. Steiner, N. A. Nwokoro, R. I. Kelley, et al. 2001. Biochemical, phenotypic and neurophysiological characterization of a genetic mouse model of RSH/Smith-Lemli-Opitz syndrome. *Hum. Mol. Genet.* **10**: 555–564.
 72. Fitzky, B. U. 2001. 7-Dehydrocholesterol-dependent proteolysis of HMG-CoA reductase suppresses sterol biosynthesis in a mouse model of Smith-Lemli-Opitz/RSH syndrome. *J. Clin. Invest.* **108**: 905–915.
 73. Fliesler, S. J., N. S. Peachey, M. J. Richards, B. A. Nagel, and D. K. Vaughan. 2004. Retinal degeneration in a rodent model of Smith-Lemli-Opitz syndrome: electrophysiologic, biochemical, and morphologic features. *Arch. Ophthalmol.* **122**: 1190–1200.
 74. Wang, Y., K. M. Sousa, K. Bodin, S. Theofilopoulos, P. Sacchetti, M. Hornshaw, G. Woffendin, K. Karu, J. Sjoval, E. Arenas, et al. 2009. Targeted lipidomic analysis of oxysterols in the embryonic central nervous system. *Mol. Biosyst.* **5**: 529–541.
 75. Waage-Baudet, H., J. M. Lauder, D. B. Dehart, K. Kluckman, S. Hiller, G. S. Tint, and K. K. Sulik. 2003. Abnormal serotonergic development in a mouse model for the Smith-Lemli-Opitz syndrome: implications for autism. *Int. J. Dev. Neurosci.* **21**: 451–459.